BIOCHEMISTRY
including biophysical chemistry & molecular biology

ARTICLE

pubs.acs.org/biochemistry

Thermodynamic and Structural Properties of the Acid Molten Globule State of Horse Cytochrome *c*

Shigeyoshi Nakamura,[†] Yasutaka Seki,[‡] Etsuko Katoh,[§] and Shun-ichi Kidokoro*[,†]

[†]Department of Bioengineering, Nagaoka University of Technology, 1603-1 Kamitomioka, Nagaoka, Niigata 940-2188, Japan

[‡]School of Pharmacy, Iwate Medical University, 2-1-1 Nishitokuta, Yahaba, Iwate 028-3694, Japan

[§]Division of Plant Sciences, National Institute of Agrobiological Sciences, 2-1-2 Kannondai, Tsukuba, Ibaraki 305-8602, Japan

ABSTRACT: To understand the stabilization, folding, and functional mechanisms of proteins, it is very important to understand the structural and thermodynamic properties of the molten globule state. In this study, the global structure of the acid molten globule state, which we call MG1, of horse cytochrome *c* at low pH and high salt concentrations was evaluated by solution X-ray scattering (SXS), dynamic light scattering, and circular dichroism measurements. MG1 was globular and slightly (3%) larger than the native state, N. Calorimetric methods, such as differential scanning calorimetry and isothermal acid-titration calorimetry, were used to evaluate the thermodynamic parameters in the transitions of N to MG1 and MG1 to denatured state D of horse cytochrome *c*. The heat capacity change, ΔC_p, in the N-to-MG1 transition was determined to be 2.56 kJ K^{-1} mol^{-1}, indicating the increase in the level of hydration in the MG1 state. Moreover, the intermediate state on the thermal N-to-D transition of horse cytochrome *c* at pH 4 under low-salt conditions showed the same structural and thermodynamic properties of the MG1 state in both SXS and calorimetric measurements. The Gibbs free energy changes (ΔG) for the N-to-MG1 and N-to-D transitions at 15 °C were 10.9 and 42.2 kJ mol^{-1}, respectively.

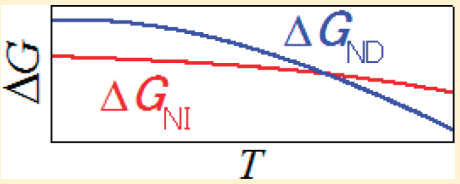

One of the goals of biophysics is to understand how the specific three-dimensional conformation of protein is spontaneously folded. A hierarchical folding funnel model was proposed to explain the folding mechanism of small proteins. The equilibrium molten globule (MG) state was reported in several globular proteins, such as cytochrome *c* and α-lactalbumin.[1−5] It was reported that this equilibrium MG state was identical to the transient folding intermediate observed in kinetic refolding, mainly by spectroscopic methods.[4−8] Moreover, it has been known that the intrinsically disordered proteins (IDPs), which have partial unfolding regions including MG-like structure, have some important functions accompanying protein−protein, protein−DNA or −RNA, and protein−lipid interactions.[9−11] Therefore, the structure and stability of the molten globule state are very important for understanding the folding, stabilization, and functional mechanisms of proteins.

Horse cytochrome *c* is a small globular protein of 104 residues with a heme region. Its equilibrium intermediate state was one of the first examples of acid MG states at low pH with a high concentration of KCl.[1] The equilibrium MG states of cytochrome *c* were reported under special solution conditions, such as a low pH and a high salt concentration.[1,12,13] Ohgushi et al. revealed that (1) the quantity of the α-helix of the MG state, which we call MG1, is identical to that of the native (N) state from CD, (2) the MG state is as compactly folded as the N state from the light scattering measurements, and (3) on the other hand one-dimensional ^{1}H NMR spectra of the MG state have the characteristics of the random coil state, indicating the rigid side chain packing is lost. Hydrogen-exchange NMR spectroscopy showed that the MG state of cytochrome *c* has strongly protected amide protons in three major helices (N-terminal, 60s, and C-terminal helices), while many other amide protons involved in tertiary structure hydrogen bonds in the N state are only marginally protected in the MG state.[12] The global structure, such as the size and shape, of the MG state is slightly expanded, but globular as determined by solution X-ray scattering.[14]

CD measurements revealed another acid MG state, which we call MG2, in the thermal transition from MG1 to the D state at a low pH with a high concentration of KCl.[15] The secondary structure of the MG2 state was identical to that of MG1, and the tertiary structure of the MG2 state was more disordered than that of the MG1 state. In a recent study, the ClO_4^--induced MG state was observed at a low pH with a high concentration of ClO_4^- at a low temperature based on CD measurement.[16] The far-UV CD spectra of the ClO_4^--induced MG at low temperature are identical to those of the N state. On the other hand, the intensity of near-UV CD of the ClO_4^--induced MG state was more suppressed than that of the MG1 state, indicating that the tertiary packing was more disordered.

The alkali MG state of cytochrome *c* was reported at alkaline pH with a high salt concentration.[17−20] Although the secondary structure of the alkali MG state was identical to that of N, the hydrodynamic radius, R_H, of alkali MG was ∼20% larger than that of the N state.

The MG states of cytochrome *c* were reported under special solution conditions, such as an acidic pH and a high salt

Received: November 10, 2010
Revised: March 8, 2011
Published: March 10, 2011

ACS Publications © 2011 American Chemical Society

concentration,[1,12,13] an alkaline pH and a high salt concentration,[17−20] a low concentration of denaturant, alcohol, or surfactant,[21−25] and acetylation of the side chain of lysine residues at low pH.[26] The MG state of the mutant yeast cytochrome *c* was observed at neutral pH by site-directed mutagenesis to rupture the hydrogen bond of the two ω-loops.[16] Recently, the equilibrium acid MG state of authentic cytochrome *c* under a native condition, in which the native state exists stably at low temperature, has been indicated in the thermal N-to-D transition of cytochrome *c* by precise calorimetry and CD measurement.[27]

Differential scanning calorimetry (DSC) of the thermal transition from the acid MG to the D state is one of the best ways to elucidate the thermodynamic stability of these MG states. While the MG state of α-lactalbumin exhibits noncooperative thermal unfolding,[28] the acid MG state of cytochrome *c* shows the cooperative unfolding transition.[27,29,30] The stability of the MG1 state of cytochrome *c* at low pH and a high salt concentration was determined as a balance of electrostatic repulsions between positive residues, which favor the extended conformation, and opposing forces such as hydrophobic interactions, which stabilize the MG state.[26]

Although the MG1-to-D state transition of horse cytochrome *c* was initially explained as a two-state transition on the basis of DSC and isothermal titration calorimetry (ITC) data,[29,30] a circular dichroism (CD) study later showed that the intermediate state, MG2, exists in the thermal transition from MG1 to the D state.[15] The thermodynamic stability of the MG2 state has not yet been examined in detail by calorimetry. It was also confirmed that the alkali MG shows a cooperative structural transition, such as thermal unfolding, cold denaturation, or denaturant unfolding.[17−20]

Although it was difficult to evaluate the transition from the N state to the MG state by DSC because the enthalpy change was too small to induce the thermal transition, the pH-induced transition from the N state to the MG1 state of bovine cytochrome *c* was clearly evaluated by isothermal acid-titration calorimetry (IATC).[31] This N-to-MG1 transition was explained well by the two-state transition model. Recently, the MG-like intermediate state on the thermal N-to-D transition of horse cytochrome *c* was observed at pH ∼4 and under low-salt conditions, called the native conditions, by precise DSC and CD measurements.[27] The compactness of the intermediate state, which is a feature of the MG state, has not been examined until now.

It is now considered that the equilibrium MG state may correspond to the late folding intermediate of cytochrome *c*.[4,7,8] On the other hand, it was confirmed that the alkali MG state of cytochrome *c* had off-pathway status.[19,20]

In this study, the thermodynamic parameters of the thermal transition from MG1 to the D state of horse cytochrome *c* at acidic pH with a high salt condition were evaluated by DSC with the three-state model that includes MG2. To examine the thermodynamic properties of MG1 of horse cytochrome *c*, the pH-induced N-to-MG1 transition of horse cytochrome *c* was evaluated by IATC, although that of bovine cytochrome *c* was already reported previously by us.[31] Additionally, the structural properties of the MG1 state and ClO_4^--induced MG state were evaluated by CD and solution X-ray scattering (SXS) measurements. Moreover, the structural properties of the MG-like intermediate state on the thermal N-to-D transition of horse cytochrome *c* at pH ∼4 and a low ionic strength were examined via analysis of the temperature dependence of the SXS data using the thermodynamic parameters from DSC.

MATERIALS AND METHODS

Cytochrome *c* Solution. Lyophilized powder of horse cytochrome *c* (c-2506; Sigma, St. Louis, MO) was dissolved in buffer. This protein solution was dialyzed with a Spectra/Por dialysis membrane (132660; Spectrum Laboratories, Rancho Dominguez, CA), with a molecular mass cutoff of 6−8 kDa, at 4 °C for ∼1 day against 1−2 L of buffer. The protein solution was ultrafiltered with a MolCut ultra filter unit (USY-20; Advantec, Tokyo, Japan), with a molecular mass cutoff of 0.2 MDa, to remove any aggregation that may have been produced during the dialysis. The concentration of horse cytochrome *c* was determined with a UB-35 spectrophotometer (Jasco, Tokyo, Japan) using an extinction coefficient (ε_{409}) of $10.6 \times 10^4\ M^{-1}\ cm^{-1}$.

Circular Dichroism Spectroscopy. Circular dichroism (CD) experiments were performed with a J-720 spectropolarimeter (Jasco) with 2 mm and 1 cm path-length quartz cells in the temperature range of 5−95 °C. The experiments were performed with 0.07−0.45 mg mL^{-1} protein solutions. The cell temperature was controlled with a PTC-343W temperature control unit (Jasco). The CD spectra of cytochrome *c* were recorded in the far-UV region (210−255 nm), near-UV region (270−330 nm), and Soret region (370−440 nm), in the same way as in the previous study.[13]

The temperature dependencies of the molar ellipticity, $[\theta]$, at 222 and 282 nm were measured from 5 to 95 °C using a heating rate of 1 K min^{-1}. The buffer solutions used in these experiments were 50 mM glycine buffer and 500 mM KCl (pH 1.5). The normalized CD ($[\theta]^{nor}$) was calculated by

$$[\theta]^{nor}(T) = \frac{[\theta](T) - [\theta]_N(T)}{[\theta]_D(T) - [\theta]_N(T)} \quad (1)$$

where $[\theta]_N$ and $[\theta]_D$ represent the molar ellipticity of the native and denatured states determined from the baselines of the pre- and post-transition, respectively, by linear least-squares fitting of eq 2 in the low-temperature range for the native state and in the high-temperature range for the denatured state.

$$[\theta]_i = A_i(T - T_0) + B_i \quad (2)$$

where T_0 was fixed to 273.15 K in this analysis.

To examine the theoretical fitting curves, we analyzed the normalized CD ($[\theta]^{nor}$) at 222 and 282 nm simultaneously with the three-state transition model using the equation

$$[\theta]^{nor} = [\theta]_N f_N + [\theta]_I f_I + [\theta]_D f_D \quad (3)$$

where $[\theta]_N$, $[\theta]_I$, and $[\theta]_D$ are the molar ellipticities of the native (N), intermediate (I), and denatured (D) states of cytochrome *c*, respectively. $[\theta]_N$, $[\theta]_I$, and $[\theta]_D$ at 222 and 282 nm were evaluated by this analysis as a fitting parameter. f_N, f_I, and f_D were the mole fractions of the N, I, and D states of cytochrome *c*, respectively, examined by DSC measurements. The temperature dependencies of $[\theta]_N$, $[\theta]_I$, and $[\theta]_D$ at 222 and 282 nm were assumed to have linear functions.

Isothermal Acid-Titration Calorimetry. Isothermal acid-titration calorimetry (IATC) is a method for evaluating the enthalpy of protein molecules as a function of pH using isothermal titration calorimetry (ITC) and pH measurement.[31,32] Here the experiments were performed with a 0.5 mg/mL cytochrome *c* solution of 500 mM KCl. The HCl titration was measured with an isothermal titration calorimeter, the ITC unit of MCS (MicroCal, Piscataway, NJ) with a cell

volume of 1.368 mL. The titration was conducted via injections of 2, 5, and 10 μL of a 20−400 mM HCl solution in 500 mM KCl by using a 250 μL syringe. A control experiment was performed with the reference solution, a 500 mM KCl solution. The pH of the HCl titration was measured by using a glass electrode and an F23 pH meter (Horiba, Kyoto, Japan). The solution used for the pH measurements was identical to that used for the calorimetric measurements. The temperature of the titration vessel for pH measurement was kept constant in a handmade glass bath with circulating water from a VM-150 thermostated water bath (Advantec, Tokyo, Japan). IATC experiments were performed at 16, 17.5, 20, 22.5, and 25 °C. Each enthalpy function at all temperatures was analyzed by the two-state global fitting method reported previously.[31] The fitting parameter $[(\partial\Delta C_p)/(\partial \mathrm{pH})]$ can be fixed to zero to fit all the experimental data within the experimental error.

Differential Scanning Calorimetry. Differential scanning calorimetry (DSC) experiments on cytochrome *c* were performed with a VP-DSC highly sensitive differential scanning calorimeter (MicroCal). The experiments were performed using a 1.0 mg mL^{-1} cytochrome *c* solution in 50 mM glycine buffer with 200, 300, 400, 500, and 600 mM KCl (pH 2.5). Before each experiment, the solution was degassed for several minutes by aspiration with a membrane pump (ULVAC, Kanagawa, Japan) and by sonication simultaneously with the Perl Clean sonication device (Fkk, Tokyo, Japan). DSC experiments were conducted at a scanning rate of 1 K min^{-1}. In all samples, the transition was reversible, as demonstrated by repeated scans of the same sample. The heat capacity functions were analyzed by the nonlinear least-squares method with the three-state model reported previously.[32−34] In this study, $\Delta C_{p,\mathrm{MG1-D}}$ and $\Delta C_{p,\mathrm{MG1-MG2}}$ were used as fixed parameters to reduce the degrees of freedom of fitting. $\Delta C_{p,\mathrm{MG1-D}}$ was fixed to 3.6 kJ K^{-1} mol^{-1} as described in pH-Induced Transition from the N State to the MG1 State of Horse Cytochrome *c* Evaluated by Isothermal Acid-Titration Calorimetry. $\Delta C_{p,\mathrm{MG1-MG2}}$ was fixed to 0 kJ K^{-1} mol^{-1} as a first assumption.

Solution X-ray Scattering. Solution X-ray scattering (SXS) measurement was performed using the method reported previously.[35] SXS experiments were conducted at beamlines BL10C of the Photon Factory at KEK and BL40B2 of SPring-8 at JASRI in Japan. The SXS profiles were measured with a flow cell through which all of the sample solution was allowed to flow at a rate of 3 μL s^{-1}. The measurement time was 10 min. The X-ray wavelengths were 0.1488 nm (BL10C, Photon Factory) and 0.1 nm (BL40B2, SPring-8). The sample-to-detector distances were ~0.8 m (BL10C, Photon Factory) and 1 m (BL40B2, SPring-8). The scattering angle was calibrated with the position of layers from the collagen fiber. The temperature of the cell holder was controlled at 10−85 °C via circulation of temperature-controlled water from a thermostat water bath. The temperature of the sample cell was measured with a thermocouple that contacted the sample cell. Protein concentrations were varied from 0 to 17 mg mL^{-1} at pH 2.5, 4, and 7 with or without salt, KCl, or $NaClO_4$. The sample and reference solutions were degassed for several minutes by aspiration with a membrane pump and by sonication simultaneously with the sonication device. To examine the thermal transition of cytochrome *c* at pH 4, we performed the SXS experiments at several temperatures (22.1−84.4 °C) with a 10 mg mL^{-1} cytochrome *c* solution. The SXS profiles were extrapolated to infinite dilution using the SXS profiles of 0−17 mg mL^{-1} protein solutions at 21.0, 68.4, and 84.7 °C.

The SXS profile was analyzed by the method reported previously.[35] When the protein concentration, *c*, is sufficiently low for the effect of the spatial correlation between protein molecules to be negligible, the SXS profile for the protein $[I(K,c)]$ is represented by the equation

$$I(K,c) = \tilde{K}M(\Delta z)^2 I_n(K) \quad (4)$$

where M is the molecular mass of the protein. K is the absolute value of the scattering vector defined as $K = (4\pi/\lambda)\sin(\theta/2)$, where λ is the wavelength of the incident X-ray and θ is the scattering angle. $\tilde{K}$ is a constant defined by the Thomason factor, Avogadro's number, the detector distance, the thickness of the sample, and the intensity of the incident X-ray. The function $I_n(K)$ is the normalized scattering factor of the protein, where $I_n(0) = 1$.

The quantity Δz is the excess number of electrons per unit weight of the protein defined by the equation

$$\Delta z = z - \rho\nu_p \quad (5)$$

where z is the number of electrons per unit weight of the protein, ρ is the mean number density of electrons in the solvent, and ν_p is the partial specific volume of the protein. The SXS profile extrapolated to infinite dilution, $I(K)$, is evaluated from a series of scattering data of the different protein concentrations.

In this study, the SXS profiles of the thermal transition of cytochrome *c* at pH 4 were analyzed with the three-state model. The SXS profile as a function of temperature is represented by the equation

$$I(K,T) = \tilde{K}M\sum_i f_i(T)[\Delta z_i(T)]^2 I_{n,i}(K) \quad (6)$$

where $f_i(T)$ and $\Delta z_i(T)$ show the temperature functions of the mole fraction and Δz of each state, respectively: the native (N), intermediate (I), and denatured (D) states of cytochrome *c*. $f_i(T)$ was determined by DSC measurements. In this study, it was assumed that the $I_n(K)$ of each state was independent of temperature. It was confirmed that the $I_n(K)$ of the native state of cytochrome *c* was independent of temperature (see Figure 6). The mean squared radius, R_{sq}, and the forward scattering intensity, $I(0)$, of the native state and the molten globule state of proteins are determined by the Guinier analysis from the SXS profile. Those values of the denatured states of proteins are determined from the SXS profile by Debye analysis. Distance distribution functions, $P(r)$, were calculated with GNOM.[36]

Density Measurement. All densities of the solutions were measured at 25 °C by using a DMA5000 high-precision vibrating tube densimeter (Anton Paar). Air and pure water were used in the calibration of the densimeter as indicated by the manufacturer.

The partial specific volume (ν_p) of the protein was calculated by using the following equations

$$d_s = \frac{1}{\nu_s} \quad (7)$$

$$\nu_s = (\nu_p - \nu_b)f_p + \nu_b \quad (8)$$

where d_s is the density of the solution, ν_s, ν_b, and ν_p are the specific volumes of the solution and buffer and the partial specific volume of the protein, respectively, and f_p is the mass fraction of the protein. The density was measured with a 0−10 mg mL^{-1} protein solution.

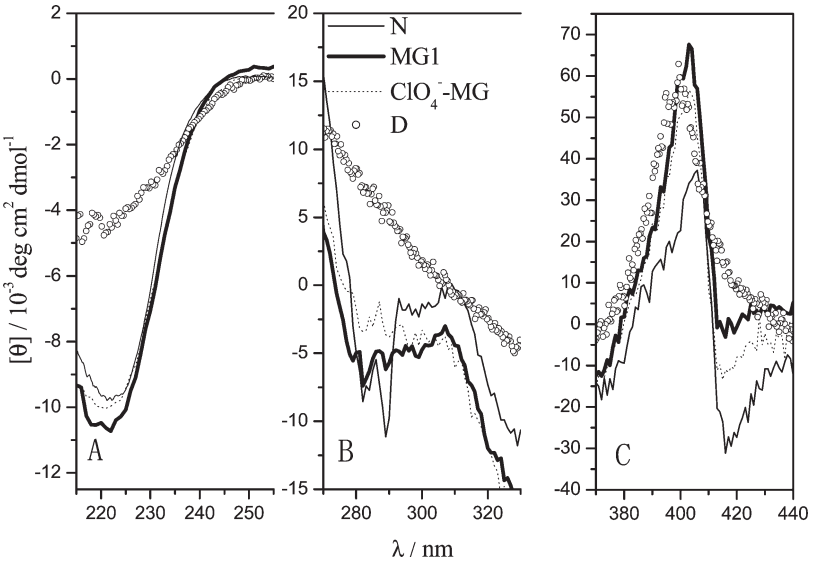

Figure 1. CD spectra of far-UV (A), near-UV (B), and Soret (C) regions of horse cytochrome *c*. Thin lines show the CD spectra of the N state (pH 4.0 and 15 °C). Thick lines and dashed lines show the CD spectra of MG1 (pH 2.5, 200 mM KCl, and 15 °C) and ClO_4^--induced MG (pH 2.5, 80 mM $NaClO_4$, and 15 °C), respectively. Empty circles show the CD spectra of the D state (pH 4.0 and 95 °C).

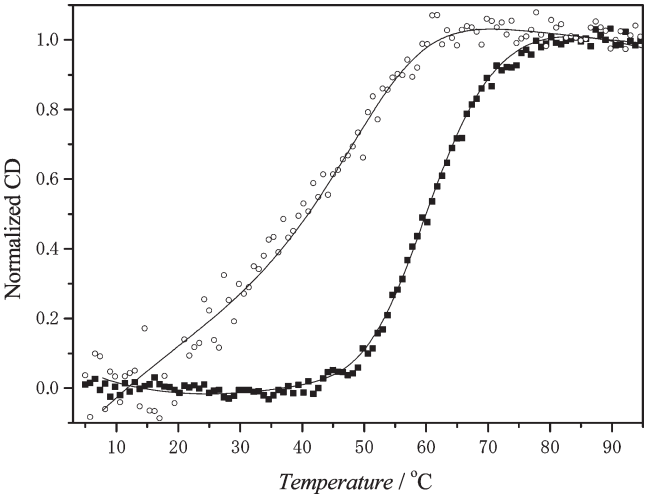

Figure 2. Temperature dependence of normalized CD at 222 nm (■) and 282 nm (○) in the transition from the MG1 state to the D state of horse cytochrome *c* at pH 2.5 in 500 mM KCl. Solid lines show the theoretical fitting curves calculated by three-state analysis using thermodynamic parameters from DSC measurements.

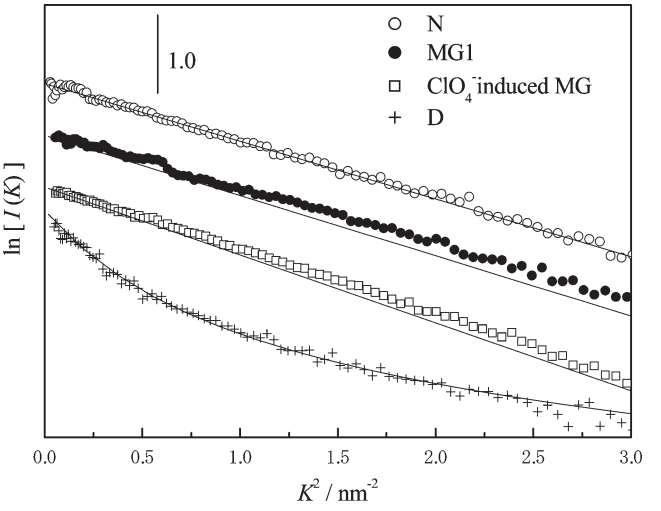

Figure 3. Guinier plots of several states of cytochrome *c*: (○) N (pH 7.0 and 25 °C), (●) MG1 (pH 2.5 and 200 mM KCl), (□) ClO_4^--induced MG (pH 2.5 and 80 mM $NaClO_4$), and (+) D (pH 4.0 and 85 °C). Solid lines show the theoretical profiles obtained from the least-squares fit of the Guinier and Debye formulas to the experimental ones.

Dynamic Light Scattering Measurement. Dynamic light scattering (DLS) measurements were performed by using a Zetasizer NanoZS (Malvern Instruments).[37] The DLS measurements were performed at 15 °C with 1−2 mg mL^{-1} protein solutions. All samples were filtered through a 0.22 μm pore size membrane before the measurements. The hydrodynamic radii (R_H) of the N state (pH 4) and MG1 (pH 2.5, 200 mM KCl) of cytochrome *c* were calculated using the Einstein−Stokes relation.

■ RESULTS

CD Measurements of the Acid Molten Globule State of Cytochrome *c*. Figure 1 shows the CD spectra of the N (pH 4.0 and 15 °C), MG1 (pH 2.5, 200 mM KCl, and 15 °C), ClO_4^--induced MG (pH 2.5, 80 mM $NaClO_4$, and 15 °C), and D (pH 4.0 and 95 °C) states. In the far-UV region, the CD spectra of the MG1 state and the ClO_4^--induced MG state agree almost totally with that of the N state, indicating that the α-helix contents of MG1 and ClO_4^--induced MG are identical with that of the N state.

In the near-UV region, the CD spectra of the N state show two negative peaks, at 282 and 289 nm, derived from the side chain packing of the tryptophan residue of the protein molecule. These two peaks disappear in the CD spectra of the D state, indicating that this side chain packing of tryptophan residue was lost in the D state. Although the near-UV CD spectra of MG1 and ClO_4^--induced MG are close to that of N, there are clear distinctions between that of N and those of these MG states. The results indicate that the

dx.doi.org/10.1021/bi101806b |*Biochemistry* 2011, 50, 3116–3126

Table 1. Forward Scattering Intensities $[I(0)]$ and Mean Square Radii (R_{sq}) of Horse Cytochrome *c* Evaluated by SXS and Partial Specific Volumes (ν_p) and Densities of the Solvent (d_b) Determined by Density Measurements at 25 °C

pH	salt concentration (mM)	T (°C)	$I(0)^{a,b}$	$R_{sq}{}^{b}$ (nm)	$I(0)^{a,c}$	$R_{sq}{}^{c}$ (nm)	$D_{max}{}^{c}$ (nm)
7.0	–	25.7	1.00 ± 0.01	1.49 ± 0.02	1.00 ± 0.01	1.43 ± 0.01	3.7
4.0	–	21.0	1.000 ± 0.004	1.48 ± 0.01			
4.0	–	84.7	0.90 ± 0.04	2.9 ± 0.2			
2.5	200 mM KCl	12.4	0.86 ± 0.01	1.52 ± 0.01	0.85 ± 0.01	1.48 ± 0.03	4.3
2.5	500 mM KCl	12.4	0.71 ± 0.01	1.49 ± 0.01			
2.5	80 mM $NaClO_4$	12.5	1.20 ± 0.01	1.61 ± 0.01	1.17 ± 0.01	1.56 ± 0.02	4.6

pH	salt concentration (mM)	ν_p (mL g^{-1})	d_b (g mL^{-1})
7.0	–	0.72 ± 0.02	(1.004884 ± 1) × 10^{-6}
4.0	–	0.740 ± 0.002	
4.0	–		
2.5	200 mM KCl	0.74 ± 0.02	(1.008413 ± 1) × 10^{-6}
2.5	500 mM KCl	0.73 ± 0.02	(1.022207 ± 1) × 10^{-6}
2.5	80 mM $NaClO_4$	0.680 ± 0.001	(1.006592 ± 1) × 10^{-6}

[a] The forward scattering intensity, $I(0)$, is normalized by $I(0)$ at pH 7.0. [b] $I(0)$ and R_{sq} evaluated via Guinier analysis. [c] $I(0)$, R_{sq}, and D_{max} evaluated via $P(r)$ function analysis.

specific side chain packing of the tryptophan residue of the MG1 and ClO_4^--induced MG state remains, but the order of the structure is more reduced than that of the N state. This also indicates that the specific side chain packing of the tryptophan residue of the ClO_4^--induced MG is more disordered than that of the MG1 state.

In the Soret region, the CD spectrum of the N state shows a large negative peak of the Cotton effect at 416 nm, derived from the interactions between Met-80 and the heme region.[16] This negative peak at 416 nm disappears in the CD spectra of the MG1, ClO_4^--induced MG, and D states, indicating that the interactions between Met-80 and the heme region were lost in the MG1, ClO_4^--induced MG, and D states. These results for the CD spectra agree closely with those of the previous report.[13]

Figure 2 shows the temperature dependence of the normalized CD at 222 and 282 nm in the thermal transition of horse cytochrome *c* at pH 2.5 in 500 mM KCl. The normalized CD at 282 nm increased over a lower temperature range than that at 222 nm. This discrepancy indicates the existence of at least one intermediate state (MG2) in the thermal MG1-to-D transition of horse cytochrome *c*. This is consistent with a previous report.[15]

The theoretical fitting curves were calculated on the basis of the thermodynamic parameters from DSC measurement, which are shown later. They agreed with the measurement data very well. This indicated that the thermodynamic parameters of the three-state model are consistent with the CD data in this figure.

Solution X-ray Scattering Profile of the Acid Molten Globule State of Cytochrome *c* at Low pH and a High Anion Concentration. Guinier plots of the SXS profile give the forward scattering intensity, $I(0)$, and the mean square radius, R_{sq}, which is clear information about the size or compactness of the protein molecule in solution. Figure 3 shows the Guinier plots of SXS profiles in the N (pH 4.0 and 21 °C), MG1 (pH 2.5, 200 mM KCl, and 12 °C), ClO_4^--induced MG (pH 2.5, 80 mM $NaClO_4$, and 12 °C), and D (pH 4.0 and 85 °C) states of cytochrome *c*. In the appropriate *K* range (for the N and MG states, $KR_{sq} < 1.1$; for the D state, $KR_{sq} < 2.0$), all experimental data were approximated well by the fitting curves.

The $I(0)$ and R_{sq} values of horse cytochrome *c* are listed in Table 1. The R_{sq} values of the N state at pH 4.0 and 7.0 are identical within experimental error, indicating that the solvent pH does not influence the R_{sq} of the N state. The R_{sq} of the MG1 state at pH 2.5 in 200 mM KCl and that in 500 mM KCl almost agree. The R_{sq} of MG1 is almost identical to that of the N state of cytochrome *c*. In particular, this indicates that MG1 is slightly (3%) larger than the N state. The R_{sq} of ClO_4^--induced MG is also slightly (10%) larger than those of the N and MG1 states, but far smaller than that of the D state. The forward scattering intensities $[I(0)]$ of MG1 and ClO_4^--induced MG states are different from that of the N state. This difference in the $I(0)$ of each state is related to the excess number of electrons per unit weight of the protein, Δz, shown as eq 4. The Δz is defined by the partial specific volume, ν_p, and the mean number density of electrons in the solvent, ρ, shown as eq 5. ρ is calculated from the density of the buffer solution, d_b. The ν_p and d_b values of the N, MG1, and ClO_4^--induced MG states are listed in Table 1. The difference in $I(0)$ between the N and MG1 states can be explained by the large difference in the d_b values of the N and MG1 states. On the other hand, the main factor in the difference in $I(0)$ between the N state and the ClO_4^--induced MG state is the ν_p of ClO_4^--induced MG, which is remarkably smaller than that of the N state.

Figure 4 shows the Kratky plots of cytochrome *c* in the N (pH 4.0 and 21 °C), MG1 (pH 2.5, 200 mM KCl, and 12 °C), ClO_4^--induced MG (pH 2.5, 80 mM $NaClO_4$, and 12 °C), and D (pH 4.0 and 85 °C) states. The Kratky plots of the N, MG1, and ClO_4^--induced MG states clearly showed the globular pattern. In particular, the Kratky plots of the N and MG1 states agreed closely. Figure 5 shows the distance distribution functions, $P(r)$, of the N, MG1, and ClO_4^--induced MG states. The $I(0)$, R_{sq}, and D_{max} values are listed in Table 1. The $I(0)$ and R_{sq} from $P(r)$ function analysis almost agree with those from Guinier analysis. The SXS profiles indicate that the global structure, the shape and size, of MG1 is almost identical to that of the N state. They also indicated that the ClO_4^--induced MG state is a compact globular conformation and that the ClO_4^--induced MG state is slightly larger than the N and MG1 states.

The hydrodynamic radii (R_H) of the N and MG1 states of cytochrome *c* were evaluated by DLS measurements. The R_H values of the N and MG1 states were 1.87 and 1.92 nm, respectively

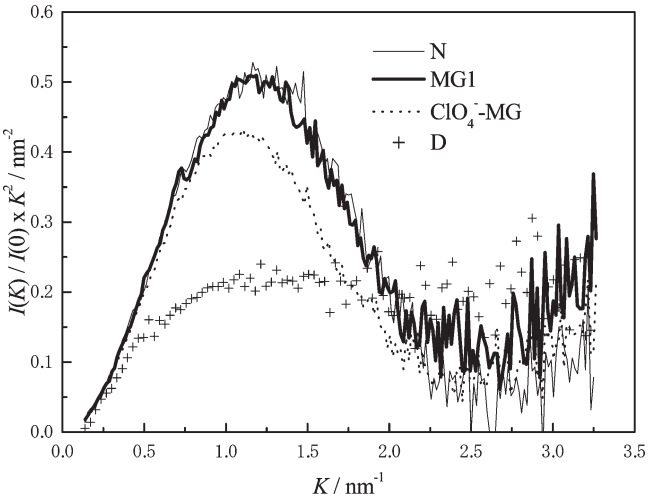

Figure 4. Kratky profiles of several states of cytochrome *c*: (thin line) N (pH 7.0 and 25 °C), (thick line) MG1 (pH 2.5, 200 mM KCl, and 12 °C), (dotted line) ClO_4^--induced MG (pH 2.5, 80 mM $NaClO_4$, and 12 °C), and (+) D (pH 4.0 and 85 °C).

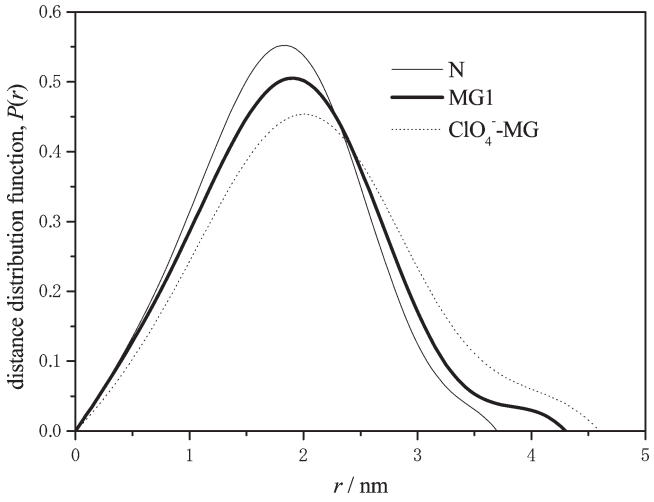

Figure 5. Distance distribution functions, $P(r)$, of several states of cytochrome *c*: (thin line) N (pH 7.0 and 25 °C), (thick line) MG1 (pH 2.5, 200 mM KCl, and 12 °C), and (dotted line) ClO_4^--induced-MG (pH 2.5, 80 mM $NaClO_4$, and 12 °C).

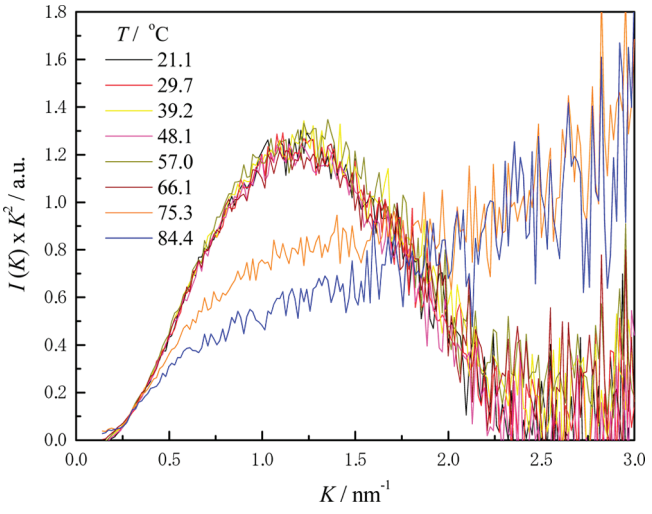

Figure 6. Kratky profiles of a 10 mg mL^{-1} cytochrome *c* solution at pH 4 from 21.1 to 84.4 °C.

(listed in Table 2). These indicate that a hydrated molecule of MG1 is slightly (3%) larger than that of the N state.

Solution X-ray Scattering Profile of the Molten Globule State of Cytochrome *c* Observed as an Intermediate State on the Thermal N-to-D Transition at pH 4 and a Low Salt Concentration. Figure 6 shows the temperature dependence of the Kratky profiles of a 10 mg mL^{-1} cytochrome *c* solution in the thermal transition from the N state to the D state. The Kratky profiles of cytochrome *c* at 21.1−39.2 °C agree very well. In the temperature range of 21.1−39.2 °C, the N state of cytochrome *c* exists stably.[27] This indicated that the temperature dependencies of the Kratky profiles of the N state were small. The Kratky profiles of cytochrome *c* at 21.1−66.1 °C exhibit a globular pattern. On the other hand, the Kratky profile at 84.4 °C exhibits the chain pattern.

The SXS profiles were extrapolated to infinite dilution with the SXS profiles of 0−17 mg/mL protein solutions at 21.0, 68.4, and 84.7 °C. The mole fraction of the N state at 21.0 °C and that of the D state at 84.7 °C were almost 1.[27] The mole fractions of the N, I, and D states at 68.4 °C were 0.29, 0.53, and 0.18, respectively. The SXS profiles of the I state were extracted from the profiles at 68.4 °C via analysis using thermodynamic parameters from the DSC measurements previously reported.[27]

Figure 7 shows the Kratky profiles of each state of cytochrome *c*. The Kratky profile was divided by $I(0)$ for normalization. The Kratky profiles of the N and I states show the typical globular pattern. On the other hand, the Kratky profiles of the D state show the chain pattern.

The height of the Kratky profile of the I state was slightly lower than that of the N state. This discrepancy is for $I(0)$ of the I state. $I(0)$ of the I state was larger than that of the N state. The ratio of $I(0)$ of the N and I states $\{[I(0)_I]/[I(0)_N]\}$ is 1.13. This suggested that the intermolecular interaction of the I state was not neglected under this measurement condition as discussed later. On the other hand, the shape of the Kratky profile of the I state was almost identical to that of the N state, suggesting that this intermediate state had a compactly globular structure like that of the N state.

pH-Induced Transition from the N State to the MG1 State of Horse Cytochrome *c* Evaluated by Isothermal Acid-Titration Calorimetry. Figure 8 shows the enthalpy function of pH in the transition from the N state to the MG1 state of horse cytochrome *c* in 500 mM KCl at 16−25 °C. Each enthalpy functions at all temperatures analyzed by the two-state global fitting method. The theoretical fitting curves well explained each experimental enthalpy function. The thermodynamic parameters at 20 °C in the pH-induced transition from the N state to the MG1 state are listed in Table 3. The $\Delta C_{p,N-MG1}$ was evaluated to be 2.56 ± 0.02 kJ K^{-1} mol^{-1} by the temperature dependence of the enthalpy change from DSC and IATC measurements (described later). Heat capacity change $\Delta C_{p,N-D}$ in the thermal transition from the N state to the D state is 6.2 ± 0.1 kJ K^{-1} mol^{-1}.[27] Therefore, heat capacity change $\Delta C_{p,MG1-D}$ in the transition from the MG1 state to the D state is estimated to be 3.6 kJ K^{-1} mol^{-1}.

Thermal Transition from the MG1 State to the D State of Cytochrome *c* Evaluated by Differential Scanning Calorimetry. Figure 9A shows the temperature dependence of the partial molar heat capacity of cytochrome *c* at pH 2.5 in 200−600 mM

Table 2. Structural Properties of Different Conformational States of Cytochrome *c*

state	$[\theta]_{222}$ (deg cm^2 dmol^{-1})	troughs of CD (280−300 nm)	chemical shift dispersion[a]
N[b]	−9731	distinct	large
MG1[c]	−10728	weak	small
ClO_4^--induced MG[d]	−9969	very weak	
D[e]	−4452	none	small

state	global structure from Kratky profile	R_{sq} (nm)	R_H (nm) from DLS analysis
N[b]	globular	1.48 ± 0.01	1.87 ± 0.01
MG1[c]	globular	1.52 ± 0.01	1.93 ± 0.03
ClO_4^--induced MG[d]	globular	1.61 ± 0.01	
D[e]	chain	2.9 ± 0.2	

[a] Chemical shift dispersion of one-dimensional ^{1}H NMR spectra of Ohgushi et al.[1] [b] At pH 4.0. [c] At pH 2.5 in 200 mM KCl. [d] At pH 2.5 in 80 mM $NaClO_4$. [e] At pH 4.0 and high temperatures.

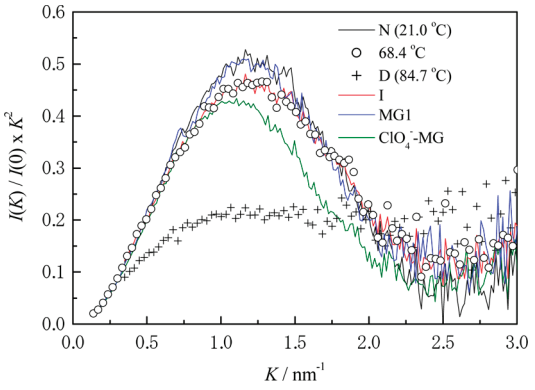

Figure 7. Kratky profiles of cytochrome *c* at pH 4, which was extrapolated to infinite dilution. The black line, empty circles, and pluses show the Kratky profiles of cytochrome *c* at 21.0 (N), 68.4, and 84.7 °C (D), respectively. The red line shows the estimated Kratky profile of the I state by the analysis of the SXS profile at 68.4 °C as described in Materials and Methods. Blue and green lines show the Kratky profiles of the MG1 (pH 2.5, 200 mM KCl, and 12 °C) and ClO_4^--induced MG (pH 2.5, 80 mM $NaClO_4$, and 12 °C) states of cytochrome *c*, respectively.

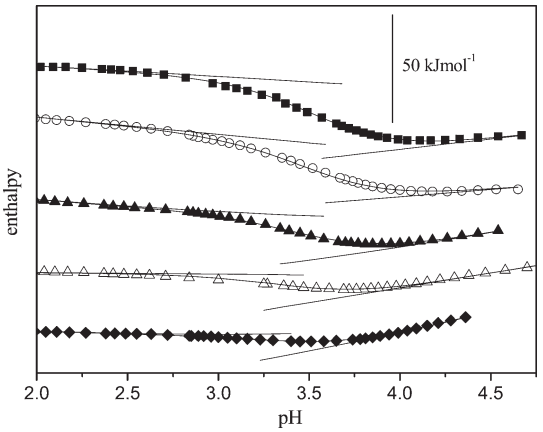

Figure 8. Enthalpy functions of pH evaluated by isothermal acid-titration calorimetry (IATC). Enthalpy functions of cytochrome *c* in the transition from the N state to the MG1 state at (◆) 16, (△) 17.5, (▲) 20, (○) 22.5, and (■) 25 °C. Solid lines show the theoretical fitting curves and baselines of the N and MG1 states calculated by the global fitting method.[31]

KCl. The endothermic peak was observed in all heat capacity functions. When the concentration of KCl was increased, the endothermic peak shifted to a higher value. The thermal transition from the MG1 state to the D state of cytochrome *c* was described by the three-state model that includes the intermediate state, MG2.[15] In this study, DSC profiles were analyzed by nonlinear least-squares fitting with two- and three-state models.

Figure 9B shows the DSC profile of cytochrome *c* at pH 2.5 and 500 mM KCl and theoretical fitting curves by two- and three-state analyses. The theoretical fitting curve of three-state analysis explained the experimental data very well. On the other hand, the systematic discrepancy between the experimental and theoretical curves remained clear.

As shown in Figure 9A, the theoretical curves calculated with the three-state model explained the experimental heat capacity function in all cases, from 200 to 600 mM KCl. The thermodynamic parameters, such as the midpoint temperature (T_m), the heat capacity change (ΔC_p), and the enthalpy change (ΔH), are listed in Table 4. In this study, the nonlinear least-squares fitting with the three-state model was performed with $\Delta C_{p,MG1-D}$ and $\Delta C_{p,MG1-MG2}$ as fixed parameters to reduce the degrees of freedom of the fitting. $\Delta C_{p,MG1-D}$ was fixed to 3.6 kJ K^{-1} mol^{-1} as described above. $\Delta C_{p,MG1-MG2}$ was fixed to 0 kJ K^{-1} mol^{-1} as the first assumption in Table 4. It was confirmed that the fitting curves could explain measurement data without large residuals when $\Delta C_{p,MG1-MG2}$ was fixed to 0−2.5 kJ K^{-1} mol^{-1}.

Figure 10 shows the temperature dependence of the mole fraction of each state in the thermal transition of cytochrome *c* at pH 2.5 in 200, 400, and 600 mM KCl. At all KCl concentrations, MG2 was observed at around $T_{m,MG1-D}$. The maximal mole fractions of MG2 in 200, 400, and 600 mM KCl were 0.21, 0.40, and 0.43, respectively.

Table 4 lists the thermodynamic parameters of the thermal transition from the MG1 state to the D state of horse cytochrome *c* at pH 2.5 and 200−600 mM KCl by DSC. $\Delta H_{MG1-MG2}$ and ΔH_{MG1-D} at 0 mM KCl were extrapolated from $\Delta H_{MG1-MG2}$ and ΔH_{MG1-D} at 200−600 mM KCl are listed in Table 5.

DISCUSSION

Structural Properties of the MG1 State of Horse Cytochrome *c*. Table 2 lists the structural properties of the MG1 state and the ClO_4^--induced MG state of horse cytochrome *c* at low pH and high anion concentrations. The CD spectra showed that

Table 3. Thermodynamic Parameters in the pH-Induced Transition from the N State to the MG1 State of Horse Cytochrome *c* at 20 °C by IATC

$pH_{d,N-MG1}$	$\Delta\nu_{N-MG1}$	ΔH_{N-MG1} (kJ mol^{-1})
3.56 ± 0.04	1.8 ± 0.1	20 ± 2
$(\partial\Delta H_{N-MG1})/(\partial pH)$ (kJ mol^{-1} pH^{-1})	$\Delta C_{p,N-MG1}$ (kJ K^{-1} mol^{-1})	$(\partial\Delta C_{p,N-MG1})/(\partial pH)$ (kJ K^{-1} mol^{-1} pH^{-1})
−15 ± 2	3.1 ± 0.4	0 (fixed)

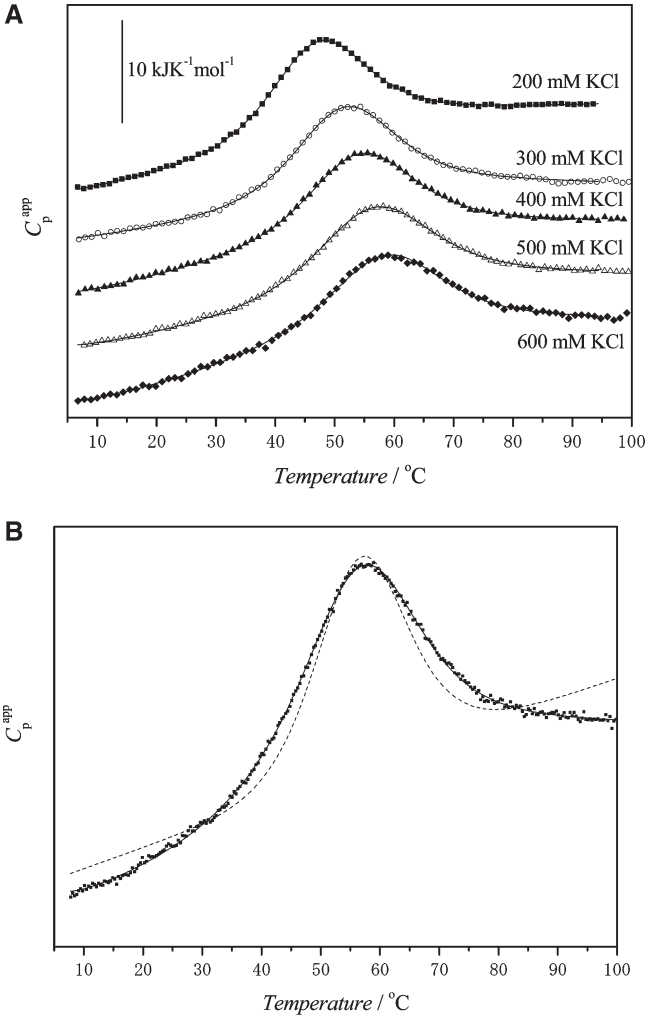

Figure 9. Temperature dependence of the partial molar heat capacity of cytochrome *c* at pH 2.5. (A) Temperature dependence of the partial molar heat capacity of cytochrome *c* at pH 2.5 in 200 (■), 300 (○), 400 (▲), 500 (△), and 600 mM KCl (◆). Solid lines show the theoretical fitting curves calculated by three-state transition analysis. (B) Temperature dependence of the partial molar heat capacity of cytochrome *c* at pH 2.5 in 500 mM KCl (■). Dashed and solid lines show the theoretical fitting curves by two-state and three-state analyses, respectively.

Table 4. Thermodynamic Parameters in the Thermal Transition from the MG1 State to the D State of Horse Cytochrome *c* at pH 2.5 by DSC

[KCl] (mM)	transition	T_m (°C)	ΔC_p (kJ K^{-1} mol^{-1})	ΔH (kJ mol^{-1})
200	MG1-to-MG2	52 ± 9	0.0 (fixed)	71 ± 40
200	MG1-to-D	44 ± 1	3.6 (fixed)	179 ± 20
300	MG1-to-MG2	51 ± 6	0.0 (fixed)	69 ± 30
300	MG1-to-D	48 ± 2	3.6 (fixed)	181 ± 20
400	MG1-to-MG2	46 ± 5	0.0 (fixed)	74 ± 15
400	MG1-to-D	49 ± 1	3.6 (fixed)	186 ± 15
500	MG1-to-MG2	53 ± 2	0.0 (fixed)	88 ± 13
500	MG1-to-D	52.6 ± 0.7	3.6 (fixed)	190 ± 13
600	MG1-to-MG2	46 ± 4	0.0 (fixed)	82 ± 11
600	MG1-to-D	52 ± 1	3.6 (fixed)	194 ± 9

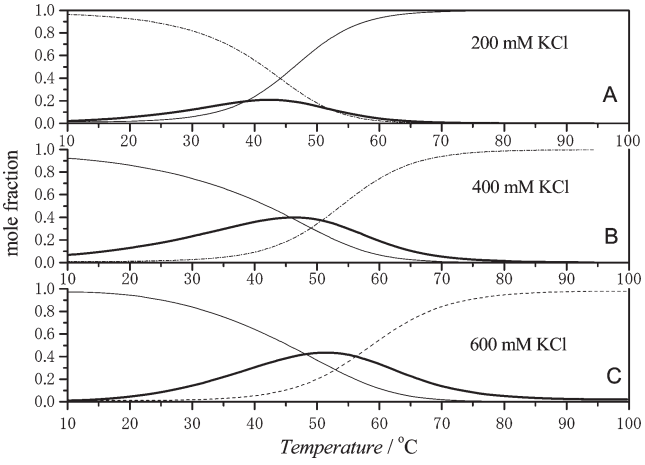

Figure 10. Temperature dependence of the mole fraction of the MG1, MG2, and D states of cytochrome *c* at pH 2.5 in 200 (A), 400 (B), and 600 mM KCl (C). Thin, thick, and dashed lines show the mole fractions of the MG1, MG2, and D states, respectively.

the α-helix content of the MG1 state (pH 2.5 and 500 mM KCl) and the ClO_4^--induced MG state are identical to that of the N state. On the other hand, the side chain packing of tryptophan residues and the heme region of the MG1 state is more disordered than that of the N state. These results were consistent with those of previous reports.[1,13] Ohgushi et al. showed one-dimensional ^{1}H NMR measurements of MG1 and suggested that the specific side chain packings of the aromatic residues of the MG1 state are more disordered than that of the N state, and that the fluctuation of the MG1 state is greater than that of the N state.[1]

The Kratky profile of the MG1 state (pH 2.5, 200 mM KCl, and 12 °C) was identical to that of the N state (pH 4.0 and 21 °C). The R_{sq} of MG1 is slightly (3%) larger than that of the N state. This strongly suggested that the global structure, the shape and size, of MG1 is almost identical to that of the N state. These results were consistent with the results of the hydrodynamic radius determined by DLS (Table 2).

Kataoka et al. reported the SXS profile of the acid MG states of several proteins, including horse cytochrome *c*, for the first time.[14] They reported that the Kratky profile of the MG state

dx.doi.org/10.1021/bi101806b |*Biochemistry* 2011, 50, 3116–3126

Table 5. Thermodynamic Parameters of the Thermal Transitions of Cytochrome *c* at 50 °C and pH 2.5

	N ⟷ MG1	MG1 ⟷ MG2	MG2 ⟷ D
ΔH (kJ mol^{-1})	113 ± 3	63 ± 16[a]	107 ± 16[a]
ΔC_p (kJ K^{-1} mol^{-1})	2.56 ± 0.02	0−2.5	1.1−3.6

[a] Thermodynamic parameters extrapolated at 0 mM KCl.

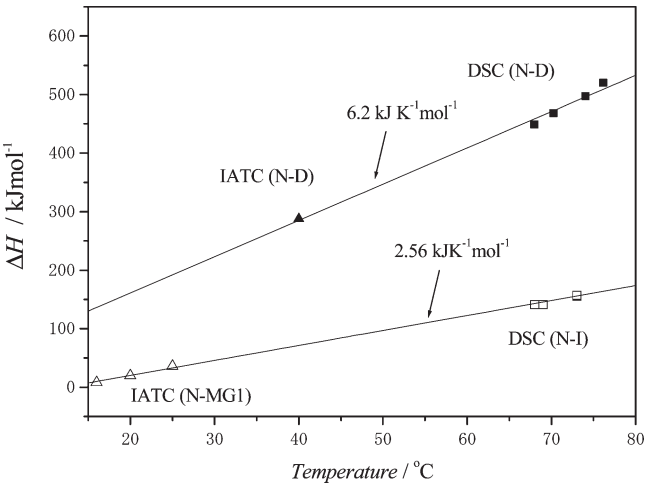

Figure 11. Temperature dependence of the enthalpy change in the structure transition of horse cytochrome *c* examined by DSC and IATC. Filled squares show the ΔH values of the N-to-D transition of horse cytochrome *c* at pH 4 examined by DSC.[27] The filled triangle shows the ΔH of the N-to-D transition examined by IATC.[27] Empty squares show the ΔH values of the N-to-I transition of horse cytochrome *c* at pH 4 examined by DSC.[27] Empty triangles show the ΔH values of the N-to-MG1 transition of horse cytochrome *c* at pH 2.5 in 500 mM KCl examined by IATC. Solid lines show the linear fitting curves of IATC and DSC results.

(pH 2.0, 500 mM NaCl, and 20 °C) of horse cytochrome *c* showed a globular pattern but differed from that of the N state (pH 7 and 20 °C). They reported that the R_{sq} values of the N, MG, and D (pH 2) states at 20 °C were 1.35, 1.74, and 2.42 nm, respectively. These values were slightly different from those in our study. Although the reason for this discrepancy is not clear, one possibility is the discrepancy in the experimental conditions between the experiments. The experiments were performed at 10 °C in our study and 20 °C in the previous study. In DSC experiments, the MG2 state was observed slightly at 20 °C and 500 mM KCl. Thus, the mixture of the MG1 and MG2 states may have been measured in the previous study. Another possibility was the slight differences in the analytical methods between these studies, especially the extrapolating method of the SXS profile to an infinite dilution.[35]

The SXS profiles of the ClO_4^--induced MG state (pH 2.5, 80 mM $NaClO_4$, and 12 °C) showed that the ClO_4^--induced MG state also had a compact globular structure. However, the Kratky profile of the ClO_4^--induced MG state was clearly different from those of the N and MG1 states. The peak of the Kratky profile was shifted to a low-angle region. The R_{sq} of the ClO_4^--induced MG state is larger than that of the N state by 10%.

In our previous study, the MG-like intermediate state, which had nativelike α-helical content and a disordered tertiary structure, was observed on the thermal N-to-D transition of horse

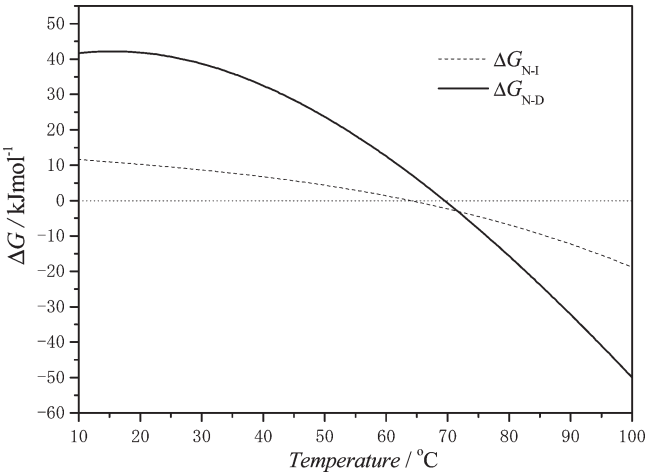

Figure 12. Temperature dependence of the Gibbs free energy change, ΔG, of cytochrome *c* at pH 4 examined by DSC[27] with $\Delta C_{p,NI}$ fixed at 2.56 kJ K^{-1} mol^{-1}. Solid and dashed lines show ΔG_{N-D} and ΔG_{N-I} values, respectively.

cytochrome *c* by DSC and CD measurements.[27] The extracted Kratky profile of this intermediate (I) state showed a compact globular pattern indicating that the I state was the molten globule state.

The Kratky profile was divided by $I(0)$ to normalize the profile. Because the $I(0)$ of the I state was larger than that of the N state, the height of the Kratky profile of the I state was slightly lower than that of the N state. There is a possibility that the intermolecular interaction, such as aggregation of the I state, occurred in SXS measurements. If aggregation of the I state occurred, the apparent $I(0)$ became larger than the true $I(0)$ value. Therefore, the $I(0)$ and R_{sq} values of the I state in this thermal transition were not evaluated precisely for the aggregation in this study. There is another possibility that the large $I(0)$ of the I state may be interpreted by the excess hydration in the I state. It was reported that the $I(0)$ of the kinetic intermediate state upon folding was larger than that of the N state by more protein hydration.[38,39] Therefore, the difference in the height of the Kratky profile of the I and N states was insignificant in this study. On the other hand, the influence of aggregation on the shape of the Kratky profile over this *K* range was not so large because the amounts of aggregation were very small. The shape and position of the peak of the Kratky profile of the I state were almost the same as those of the N and MG1 states. These were clearly different from the shape of the Kratky profile of the ClO_4^--induced MG state. This suggested that this intermediate state of the thermal N-to-D transition at pH 4 had structural properties similar to those of the MG1 state.

The hydrodynamic radii (R_H) of the N state and the alkali molten globule state determined by pulsed-field-gradient NMR diffusion measurements were reported.[19] The R_H of the alkali molten globule is 20% larger than that of the N state. In our study, the R_H values of the N and MG1 states were determined to be 1.87 and 1.93 nm, respectively. The R_H of the N state was consistent with the previous report.[19] The R_H of the MG1 state is slightly (3%) larger than that of the N state in our study. It was consistent with the SXS results and the previous light scattering results.[1] It was suggested that the molecular size, including the hydration of MG1, was close to that of the N state, in contrast to the case of the alkali molten globule state.

Thermodynamic Parameters of the Transition from the N State to the MG1 State of Horse Cytochrome *c*. The transitions from the N state to the MG1 state of horse cytochrome *c* were directly observed by isothermal acid-titration calorimetry (IATC) in 500 mM KCl at 16−25 °C. The ΔH at 20 °C and the ΔC_p were 20 kJ mol^{-1} and 3.1 kJ K^{-1} mol^{-1}, respectively. This property of a small enthalpy change in the N-to-MG1 transition was consistent with the ΔH of bovine cytochrome *c* evaluated by IATC reported previously.[31] The ΔC_p of the N-to-MG transition of bovine cytochrome *c* was determined to be 1.1 kJ K^{-1} mol^{-1} by global fitting at 20−35 °C. Previous data included not only the N-to-MG1 transition but also the N-to-MG2 transition because the MG2 state existed stably at 35 °C. In this study of horse cytochrome *c*, the experiments were performed at 16−25 °C to evaluate the N-to-MG1 transition precisely. Of course, this discrepancy was also due to the difference between bovine and horse cytochrome *c*.

Figure 11 shows the temperature dependence of ΔH of horse cytochrome *c* by DSC and IATC. The ΔC_p of the N-to-D transition was determined to be 6.2 kJ K^{-1} mol^{-1} by DSC and IATC data.[27] The ΔH of the N-to-MG1 transition determined by IATC and that of the N-to-I transition determined by DSC[27] are plotted simultaneously in Figure 11. The SXS experiments suggested that the intermediate state of the thermal N-to-D transition at pH 4 had MG1 state-like structure. The ΔH values of the N-to-MG1 and N-to-I transitions were analyzed simultaneously by linear fitting. The linear fitting curve explained the N-to-MG1 transition very well. The ΔC_p of the N-to-MG1 transition was determined to be 2.56 kJ K^{-1} mol^{-1}. This ΔC_p value was consistent with the $\Delta C_{p,\mathrm{N-MG1}}$ from IATC and the previous estimation of $\Delta C_{p,\mathrm{N-I}}$ (0−3 kJ K^{-1} mol^{-1} determined by DSC[27]). This indicated that this intermediate state on the thermal N-to-D transition at pH 4 had thermodynamic properties similar to those of the MG1 state. Table 5 lists the thermodynamic parameters of the thermal transition of horse cytochrome *c* at 50 °C and pH 2.5 evaluated by DSC and IATC.

In this study, $\Delta C_{p,\mathrm{N-MG1}}$ was determined to be 2.56 kJ K^{-1} mol^{-1}. This $\Delta C_{p,\mathrm{N-MG1}}$ indicates that the extent of hydrophobic hydration is increased or the extent of hydrophilic hydration is decreased in the MG1 state. Although the global structure of the MG1 state was almost identical to that of the N state from SXS measurements, the side chain packing was largely lost and the R_{sq} of the MG1 state was 3% larger than that of the N state. These results may suggest that the hydration profile is largely affected by the slight increase in the R_{sq} value. In particular, the CD experiments showed that the side chain packing of the heme region of the MG1 state is more disordered than that of the N state. It was possible that the hydration of the strong hydrophobic region, such as the heme region, had a strong influence on $\Delta C_{p,\mathrm{N-MG1}}$. The second possibility for the heat capacity increase may be the dehydration of the anions that bind the MG1 state as it was suggested that approximately two chloride ions are bound in the structural change from the N state to the MG1 state.[15] The third possibility may be the abnormal heat capacity derived from the conformational change of the MG state that has more freedom for the side chain conformation than the native state and retains ordered structures. Although the discussion of the correspondence between the structural and hydration features suggested in this study may require detailed structural simulations of the MG1 state in the future, it is very interesting that such a small increase in the R_{sq} value can produce the large structural effect.

While the previous study estimated the ΔC_p of the N-to-I transition at pH 4 to be 0−3 kJ mol^{-1} K^{-1}, in this study, this ΔC_p was determined to be 2.56 kJ K^{-1} mol^{-1} by DSC and IATC. Figure 12 shows the temperature dependence of the ΔG values of the N-to-D and N-to-I transitions of horse cytochrome *c* at pH 4 and a low salt concentration. The ΔG values of the N-to-I ($\Delta G_{\mathrm{N-I}}$) and N-to-D ($\Delta G_{\mathrm{N-D}}$) transitions at 15 °C were 10.9 and 42.2 kJ mol^{-1}, respectively. Latypov et al. reported that $\Delta G_{\mathrm{N-I}}$ and $\Delta G_{\mathrm{N-D}}$ at 15 °C and pH 5 were 8.4 and 41.0 kJ mol^{-1}, respectively, as determined by the three-state analysis of the GuHCl-induced N-to-D transition of cytochrome *c* using a spectroscopic method.[40] These results mostly agree with our results at 15 °C, pH 4, and a low salt concentration, called the native condition. At a low temperature, the native state of cytochrome *c* exists stably under the native condition, such as pH 4 and a low salt concentration. At 70 °C, the molten globule, MG1, state was observed stably under the native condition. Moreover, this molten globule state, MG1, was more stable than the denatured state by 30 kJ mol^{-1} at 15 °C under the native condition. Therefore, this MG1 state observed under the native condition should be affected by the stabilization and folding mechanisms of the native state of cytochrome *c*. However, we have no information about whether this MG state exists on the folding pathway. Bhuyan performed kinetic experiments with the alkali molten globule state of cytochrome *c* and concluded that the alkali MG state had off-pathway status.[19,20] The detailed kinetic experiments such as those described previously[19,20] should require an examination of on- versus off-pathway status of the MG1 state under the native condition.

AUTHOR INFORMATION

Corresponding Author

*Department of Bioengineering, Nagaoka University of Technology, 1603-1 Kamitomioka, Nagaoka, Niigata 940-2188, Japan. Phone and fax: +81-258-47-9425. E-mail: kidokoro@nagaokaut.ac.jp.

Funding Sources

This work was supported by Grants-in-Aid from the Ministry of Education, Culture, Sports, Science, and Technology (MEXT) of Japan. S.N. was supported by a fellowship from the Japan Society for the Promotion of Science to Young Scientists.

ACKNOWLEDGMENT

The synchrotron radiation experiments were performed at BL40B2 of SPring-8 with the approval of the Japan Synchrotron Radiation Research Institute (JASRI) (Proposal Nos. 2006A-1503, 2008A1014) and the BL10C of the Photon Factory with the approval of the KEK (Proposal No. 2005G305).

ABBREVIATIONS

MG, molten globule; N, native; D, denatured; I, intermediate; DSC, differential scanning calorimetry; ITC, isothermal titration calorimetry; IATC, isothermal acid-titration calorimetry; CD, circular dichroism; SXS, solution X-ray scattering; $P(r)$, distance distribution function; R_{sq}, mean squared radius; DLS, dynamic light scattering; R_H, hydrodynamic radius.

REFERENCES

(1) Ohgushi, M., and Wada, A. (1983) 'Molten-globule state': A compact form of globular proteins with mobile side-chains. *FEBS Lett. 164*, 21–24.

(2) Kuwajima, K. (1996) The molten globule state of α-lactalbumin. *FASEB J. 10*, 102–109.
(3) Goto, Y., Takahashi, N., and Fink, A. L. (1990) Mechanism of acid-induced folding of proteins. *Biochemistry 29*, 3480–3488.
(4) Arai, M., and Kuwajima, K. (2000) Role of the molten globule state in protein folding. *Adv. Protein Chem. 53*, 209–282.
(5) Ptitsyn, O. B. (1995) Molten globule and protein folding. *Adv. Protein Chem. 47*, 83–229.
(6) Ikeguchi, M., Kuwajima, K., Mitani, M., and Sugai, S. (1986) Evidence for identity between the equilibrium unfolding intermediate and a transient folding intermediate: A comparative study of the folding reactions of α-lactalbumin and lysozyme. *Biochemistry 25*, 6965–6972.
(7) Colon, W. C., and Roder, H. (1996) Kinetic intermediates in the formation of the cytochrome *c* molten globule. *Nat. Struct. Biol. 3*, 1019–1025.
(8) Balbach, J., Forge, V., Lau, W. S., Van Nuland, N. A., Brew, K., and Dobson, C. M. (1996) Protein folding monitored at individual residues during a two-dimensional NMR experiment. *Science 274*, 1161–1163.
(9) Fink, A. L. (2005) Natively unfolded proteins. *Curr. Opin. Struct. Biol. 15*, 35–41.
(10) Dunker, A. K., Brown, C. J., Lawson, J. D., and Iakoucheva, L. M. (2002) Intrinsic disorder and protein function. *Biochemistry 41*, 6573–6582.
(11) Dunker, A. K., Cortese, M. S., Romero, P., Iakoucheva, L. M., and Uversky, V. N. (2005) Flexible nets. The roles of intrinsic disorder in protein interaction networks. *FEBS J. 272*, 5129–5148.
(12) Jeng, M. F., Englander, S. W., Elove, G. A., Wand, A. J., and Roder, H. (1990) Structural description of acid-denatured cytochrome c by hydrogen exchange and 2D NMR. *Biochemistry 29*, 10433–10437.
(13) Santucci, R., Bongiovanni, C., Mei, G., Ferri, T., Polizio, F., and Desideri, A. (2000) Anion size modulates the structure of the A state of cytochrome c. *Biochemistry 39*, 2632–12638.
(14) Kataoka, M., Hagihara, Y., Mihara, K., and Goto, Y. (1993) Molten globule of cytochrome c studied by small angle X-ray scattering. *J. Mol. Biol. 229*, 591–596.
(15) Kuroda, Y., Kidokoro, S., and Wada, A. (1992) Thermodynamic characterization of cytochrome *c* at low pH. Observation of the molten globule state and of the cold denaturation process. *J. Mol. Biol. 223*, 1139–1153.
(16) Sinibaldi, F., Piro, M. C., Howes, B. D., Smulevich, G., Ascoli, F., and Santucci, R. (2003) Rupture of the hydrogen bond linking two ω-loops induces the molten globule state at neutral pH in cytochrome c. *Biochemistry 42*, 7604–7610.
(17) Kumar, R., Prabhu, N. P., Rao, D. K., and Bhuyan, A. K. (2006) The alkai molten globule state of horse ferricytochrome *c*: Observation of cold denaturation. *J. Mol. Biol. 364*, 438–495.
(18) Rao, D. K., Kumar, R., Yadaiah, M., and Bhuyan, A. K. (2006) The alkali molten globule state of ferrocytochrome *c*: Extraordinary stability persistent structure, and constrained overrall dynamics. *Biochemistry 45*, 3412–3420.
(19) Bhuyan, A. K. (2010) Off-pathway status for the alkali molten globule of horse ferricytochrome *c*. *Biochemistry 49*, 7764–7773.
(20) Bhuyan, A. K. (2010) Off-pathway status of the alkali molten globule is unrelated to heme misligation and trans-pH effects: Experiments with ferrocytochrome *c*. *Biochemistry 49*, 7774–7782.
(21) Bai, Y., Sosnick, T. R., Mayne, L., and Englander, S. W. (1995) Protein folding intermediates: Native-state hydrogen exchange. *Science 269*, 192–197.
(22) Ferri, T., Poscia, A., Ascoli, F., and Santucci, R. (1996) Direct electrochemical evidence for an equilibrium intermediate in the guanidine-induced unfolding of cytochrome c. *Biochim. Biophys. Acta 1298*, 102–108.
(23) Kamatari, Y. O., Konno, T., Kataoka, M., and Akasaka, K. (1996) The methanol-induced globular and expanded denatured states of cytochrome *c*: A study by CD, fluorescence, NMR and small-angle X-ray scattering. *J. Mol. Biol. 259*, 512–523.
(24) Chattopadhyay, K., and Mazumdar, S. (2003) Stabilization of partially folded states of cytochrome c in aqueous surfactant: Effects of ionic and hydrophobic interactions. *Biochemistry 42*, 14606–14613.
(25) Qureshi, S. H., Moza, B., Yadav, S., and Ahmad, F. (2003) Conformational and thermodynamic characterization of the molten globule state occurring during unfolding of cytochromes-c by weak salt denaturants. *Biochemistry 42*, 1684–1695.
(26) Goto, Y., and Nishikiori, S. (1991) Role of electrostatic repulsion in the acidic molten globule of cytochrome c. *J. Mol. Biol. 222*, 679–686.
(27) Nakamura, S., Baba, T., and Kidokoro, S. (2007) A molten globule-like intermediate state detected in the thermal transition of cytochrome *c* under low salt concentration. *Biophys. Chem. 127*, 103–112.
(28) Dolgikh, D. A., Abaturov, L. V., Bolotina, I. A., Brazhnikov, E. V., Bychkova, V. E., Gilmanshin, R. I., Lebedev, Y. O., Semisotnov, G. V., Tiktopulo, E. I., and Ptitsyn, O. B. (1985) Compact state of a protein molecule with pronounced small-scale mobility: Bovine α-lactalbumin. *Eur. Biophys. J. 13*, 109–121.
(29) Potekhin, S., and Pfeil, W. (1989) Microcalorimetric studies of conformational transitions of ferricytochrome c in acidic solution. *Biophys. Chem. 34*, 55–62.
(30) Hamada, D., Kidokoro, S., Fukada, H., Takahashi, K., and Goto, Y. (1994) Salt-induced formation of the molten globule state of cytochrome c studied by isothermal titration calorimetry. *Proc. Natl. Acad. Sci. U.S.A. 91*, 10325–10329.
(31) Nakamura, S., and Kidokoro, S. (2005) Direct observation of the enthalpy change accompanying the native to molten-globule transition of cytochrome c by using isothermal acid-titration calorimetry. *Biophys. Chem. 113*, 161–168.
(32) Nakamura, S., and Kidokoro, S. (2004) Isothermal acid-titration calorimetry for evaluating the pH dependence of protein stability. *Biophys. Chem. 109*, 229–249.
(33) Kidokoro, S., and Wada, A. (1987) Determination of thermodynamic functions from scanning calorimetry data. *Biopolymers 26*, 213–229.
(34) Kidokoro, S., Uedaira, H., and Wada, A. (1988) Determination of thermodynamic functions from scanning calorimetry data. *Biopolymers 27*, 221–225.
(35) Seki, Y., Tomizawa, T., Hiragi, Y., and Soda, K. (2007) Global structure analysis of acid-unfolded myoglobin with consideration to effects of intermolecular coulomb repulsion on solution X-ray scattering. *Biochemistry 46*, 234–244.
(36) Svergun, D. I. (1992) Determination of the refularization parameter in indirect-transform method using perceptual criteria. *J. Appl. Crystallogr. 25*, 495–503.
(37) Shiba, K., Niidome, T., Katoh, E., Xiang, H., Han, L., Mori, T., and Katayama, Y. (2010) Plydispersity as a parameter for indicating the thermal stability of proteins by dynamic light scattering. *Anal. Sci. 26*, 659–663.
(38) Svergun, D. I., Richard, S., Koch, M. H. J., Sayers, Z., Kuprin, S., and Zaccai, G. (1998) Protein hydration in solution: Experimental observation by X-ray and neutron scattering. *Proc. Natl. Acad. Sci. U.S.A. 95*, 2267–2272.
(39) Arai, M., Ito, K., Inobe, T., Nakao, M., Maki, K., Kamagata, K., Kihara, H., Amemiya, Y., and Kuwajima, K. (2002) Fast compaction of α-lactalbumin during folding studied by stopped-flow X-ray scattering. *J. Mol. Biol. 321*, 121–132.
(40) Latypov, R. F., Cheng, H., Roder, N. A., Zhang, J., and Roder, H. (2006) Structural characterization of an equilibrium unfolding intermediate in cytochrome *c*. *J. Mol. Biol. 357*, 1009–1025.